SCIENTIFIC NOTE

ESRO SN-116

March 1971

ROCKET MEASUREMENTS OF ION AND ELECTRON DENSITIES IN THE D- & LOWER E-REGIONS NEAR SUNRISE

by

A. Pedersen

European Space Research and Technology Centre

Noordwijk, The Netherlands

&

J.A. Kane

Goddard Space Flight Center,

Greenbelt, Maryland, USA

ORGANISATION EUROPEENNE DE RECHERCHES SPATIALES

EUROPEAN SPACE RESEARCH ORGANISATION

ROCKET MEASUREMENTS OF ION AND ELECTRON DENSITIES IN THE D- & LOWER E-REGIONS NEAR SUNRISE

by

A. Pedersen[*]

European Space Research and Technology Centre

Noordwijk, The Netherlands

&

J.A. Kane

Goddard Space Flight Center,

Greenbelt, Maryland, USA

[*]When this work was done, Dr. A. Pedersen was a research associate of the National Academy of Sciences at Goddard Space Flight Center.

ORGANISATION EUROPEENNE DE RECHERCHES SPATIALES
EUROPEAN SPACE RESEARCH ORGANISATION
114, avenue Charles de Gaulle, 92-Neuilly, France

ABSTRACT

Positive-ion and electron densities were measured in the 75-110 km altitude range with the aid of two rockets launched from White Sands near sunrise. The solar zenith angles were 91° and 79°, respectively. The densities were derived from measurements made by an ion collector and from data obtained with a Faraday rotation technique capable of detecting electrons in the D-region. It has been found that, in the 80-95 km altitude range, electron detachment from negative ions takes place mainly at zenith angles of less than 91°. The source of the high positive-ion density ($N_{+} \simeq 700$ cm^{-3}) at an altitude of 75 km just before sunrise is presumed to be scattered Lyman α radiation ionising nitric oxide.

TABLE OF CONTENTS

LIST OF FIGURES

ROCKET MEASUREMENTS OF ION AND ELECTRON DENSITIES IN THE D- AND LOWER E-REGIONS NEAR SUNRISE

1. INTRODUCTION

This paper discusses the results obtained from instruments carried by two rockets launched at White Sands, New Mexico, near sunrise on the 29th August 1966. Positive-ion and electron densities were measured in the D- and lower E-regions for solar zenith angles $\chi = 91^{\circ}$ and $\chi = 79^{\circ}$.

The electron density had previously been measured during sunrise on several occasions, both by ground-based techniques[1] and by rocket-borne instruments. Discussion of these measurements, aimed at reaching conclusions about ionisation and detachment during sunrise, has been inhibited by the scarcity of data concerning ion densities. The combination of positive-ion and electron density measurements on the same rocket makes it possible to assess the total charge density and negative-ion density and thus provides a better basis for discussion.

From observations of VLF waves reflected in the ionospheric D-region during sunrise, it has been found that electron densities below an altitude of about 80 km begin to increase when the solar zenith angle decreases below $\chi = 99^{\circ}$ (Ref. 2). This could be interpreted as detachment of electrons from negative ions by visible radiation. Shorter wavelengths, in the UV, do not penetrate to altitudes below 80 km at such zenith angles.

Rocket measurements of electron densities during twilight[3,4] have led to the conclusion that some negative ions require UV radiation for detachment. Fehsenfeld et al.[5] have indicated, however, that negative-ion destruction might be the result of chemical processes rather than of direct photo-detachment.

The measurements reported here indicate that at 90 km most negative ions are detached long after ($\gtrsim$ 20 minutes) illumination by UV radiation (2550 Å). The altitude gradient of the electron-density profile measured at $\chi = 91^{\circ}$ more closely matches the gradient of the Lyman α flux calculated for the

same solar zenith angle. From these observations alone, however, it is not possible to decide which wavelength, if any, is directly responsible for the observed detachment. This point will be considered in Chapter 4.

2. EXPERIMENTAL TECHNIQUES

The ion densities were measured with an ion collector which has certain similarities to the Gerdien condenser probe. A set of parallel plates was connected electrically as indicated in Figure 1a. The advantage of such a configuration is that the stray field is small, which means that the current collection does not vary strongly with bias on the plates. To demonstrate this the current, as a function of bias referred to the plasma potential $(V-V_p)$, is compared with two Langmuir probes in Figure 1b for the case of approximately orbital limited current. These curves are experimental results from a large chamber containing a low-density plasma where the Debye length was comparable to the dimensions of the probe, but several times smaller than those of the chamber.

If ion collection is to be correct, the potential in the middle of the gap between the plates should ideally be at plasma potential. The rocket, however, is expected to be a volt or so negative with respect to the plasma potential. In order to reveal the influence of this voltage difference on the measurements the positive bias, which was referred to the rocket, was increased in a sweep going between +1.5 and +3.0 V while the negative bias was kept fixed at -1.5 V. The average potential right in front of the plates was in this way moved near to, or through the plasma potential, and made it possible to find out whether the rocket's deviation from plasma potential had any serious effect on the current collection.

When the rocket is moving through a medium at a velocity v_R that is high with respect to the ionic thermal velocity v_i, the ram effect of the rocket will dominate the measured ion current. For the case of a pure ram current we can write:

$$i_+ = N_+ \, e \, v_R \, A \cos \theta$$

where

i_+ = positive current collected

N_+ = positive-ion density

v_R = rocket velocity

A = probe area (corresponds to open area of frame in Fig. 1a)

θ = angle of attack

In the collision-dominated region below 80 km, the shock wave will tend to sweep some ions past the probe so that i_+ will tend to be smaller than the

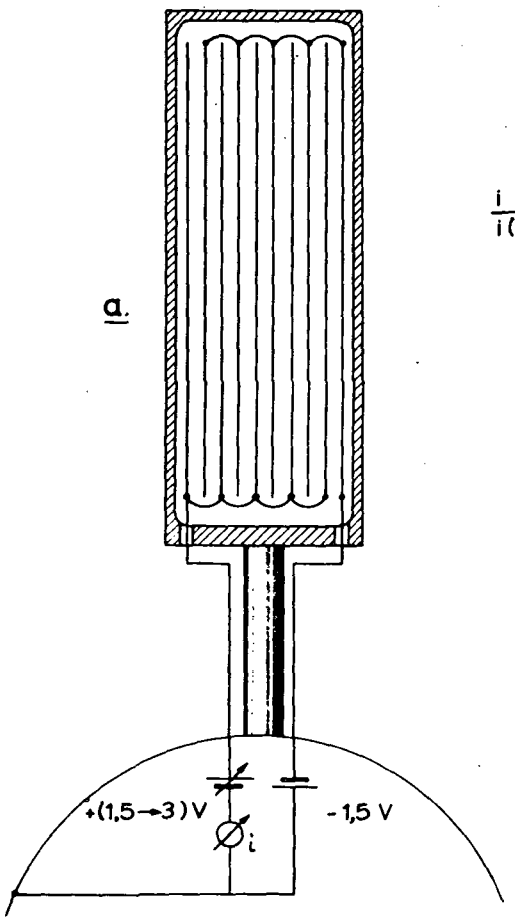

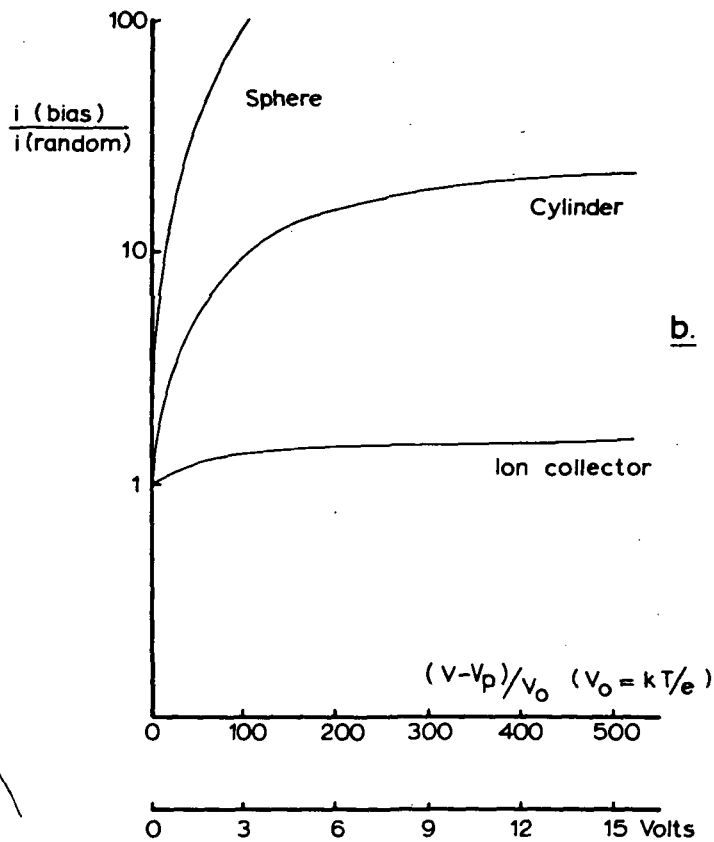

Figure 1a. Front view of the Venetian-blind ion probe, showing electrical connections of current-collecting plates, probe frame and rocket body.

Figure 1b. Experimental current (normalised to random current) v. voltage curves permitting comparison of Venetian-blind probe with cylindrical and spherical Langmuir probes.

value given by the above formula. Sonin[6] has discussed this for a probe at the blunt end of a cylinder. It seems that the corrections will be relatively small for the velocities of the rockets and the size of the probes used. The reduction factor will at the most amount to 0.5 at 70 km and be negligible at 80 km.

The electron densities were measured by means of a Faraday rotation technique using the frequencies 2.23 MHz and 3.23 MHz. Transmissions from the ground at these frequencies are received in the rocket, and the rotation of the plane of polarisation of the radio waves can be observied to yield information about the electron density distribution in the D-region. For a description of the technique, see for example Kane and Troim[7].

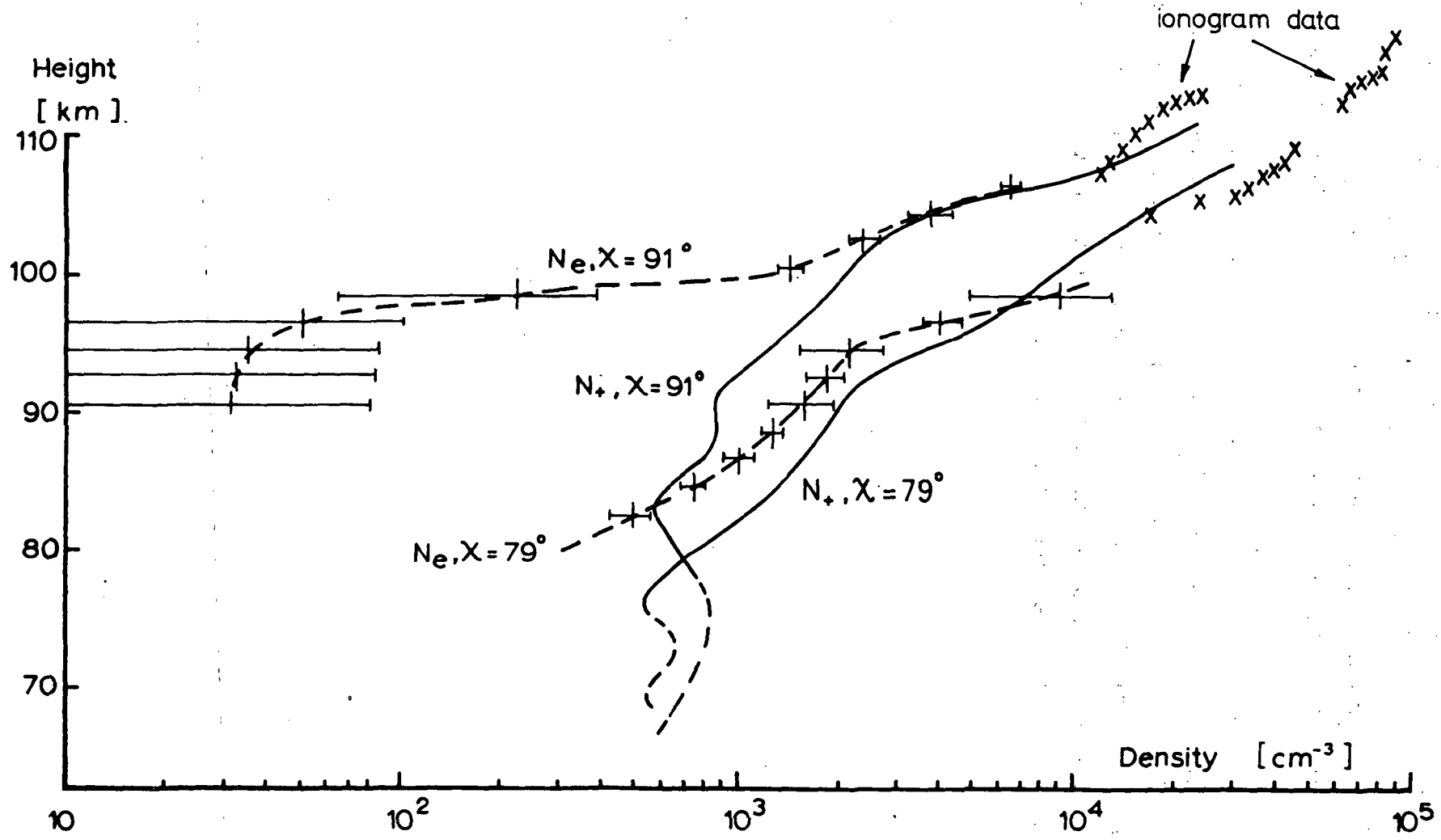

Figure 2. Electron (dots) and positive-ion (solid curves) density profiles for the two White Sands rocket shots at solar zenith angles $\chi = 91^{\circ}$ and $\chi = 79^{\circ}$. Electron densities deduced from simultaneous White Sands ionosonde data are shown as crosses.

3. RESULTS

The payloads were launched with Booster II Arcas rockets from White Sands on 29 August 1966 at 0534 and 0632 MST. The peak altitudes were 110 ± 3 and 108 ± 3 km, respectively. Because of difficulties experienced in tracking the rockets, the altitudes could only be determined to within ± 3 km. The uncertainty of one trajectory relative to the other, however, is probably not more than ± 1 km.

The positive voltage sweep on the ion collector only decreased the collected positive ion current by a small amount, of the order 10% at 70 km and 20-30% at 90 km. Near apogee, when $v_i \gtrsim v_R$, the decrease of collected positive current was about 50% for a full positive sweep. This shows that it is reasonable to assume that the collected current is nearly identical to the ram current given by the equation on page 4 when $v_i < v_R$; this condition is fulfilled throughout the flight except for a few km below peak.

Figure 2 shows the ion and electron densities for the two flights. The Faraday rotation experiment is expected to give the more reliable absolute measurements and can therefore be used as a reference for the measurement of positive-ion densities at higher altitudes where negative ions can be neglected. It can be seen from Figure 2 that there is good agreement between the measured values of electron and ion densities at the upper part of the trajectories without introducing any normalising factor on the ion current. Because of possible influences from shock waves at lower altitudes the ion density profiles are terminated at 75 km. In the region near 75 km where a comparison is possible, our N_+ values are in good agreement with the nighttime N_+ values deduced by Hale[8] from ion-conductivity measurements. The electron-density profiles shown in Figure 2 are typical of what other workers have measured at comparable zenith angles, except that the sharp altitude gradient of electron density at $\chi = 91^\circ$ seems to occur at an unusually high

altitude. This may be due in part to an error in our rocket trajectory determination, the procedure for which is given in the appendix.

From Figure 2 the corresponding values of $\lambda = N/N_e$ are shown in Figure 3. Because of the uncertainties in the N_e, N_+ measurements, the values given in Figure 3 are useful only to establish the orders of magnitude of λ for the two zenith angles involved here. Measurements of ion and electron densities using similar techniques in the auroral zone have been reported by Folkestad et al.[9] and by Jespersen et al.[10]. These authors find for nighttime auroral conditions λ values which lie between the two profiles shown in Figure 3. This conflict is presumably due to an effect of auroral particles on the negative ion detachment rate.

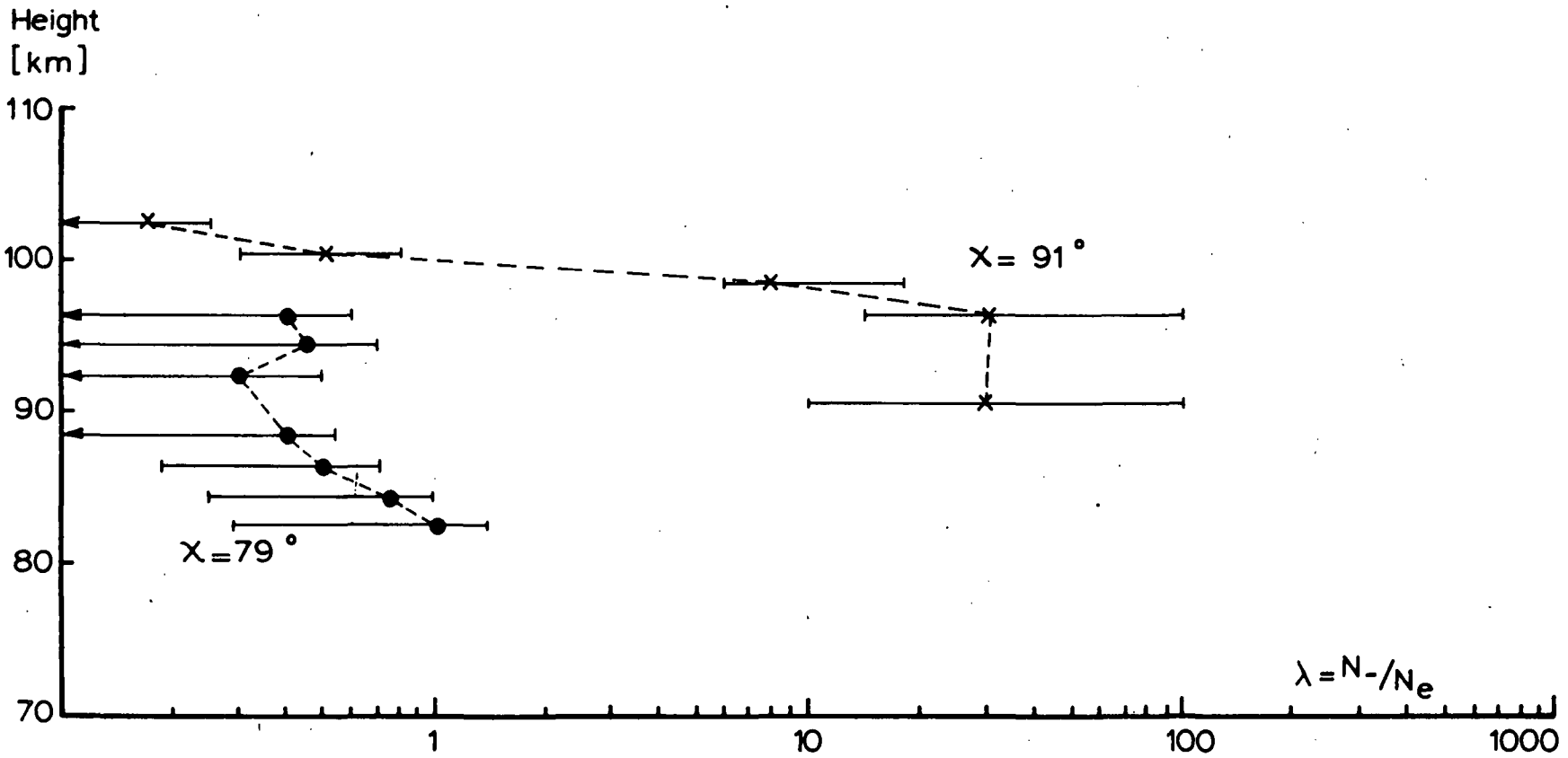

Figure 3. Altitude plot of $\lambda = \frac{N_+ - N_e}{N_e}$ derived from data of Figure 2.

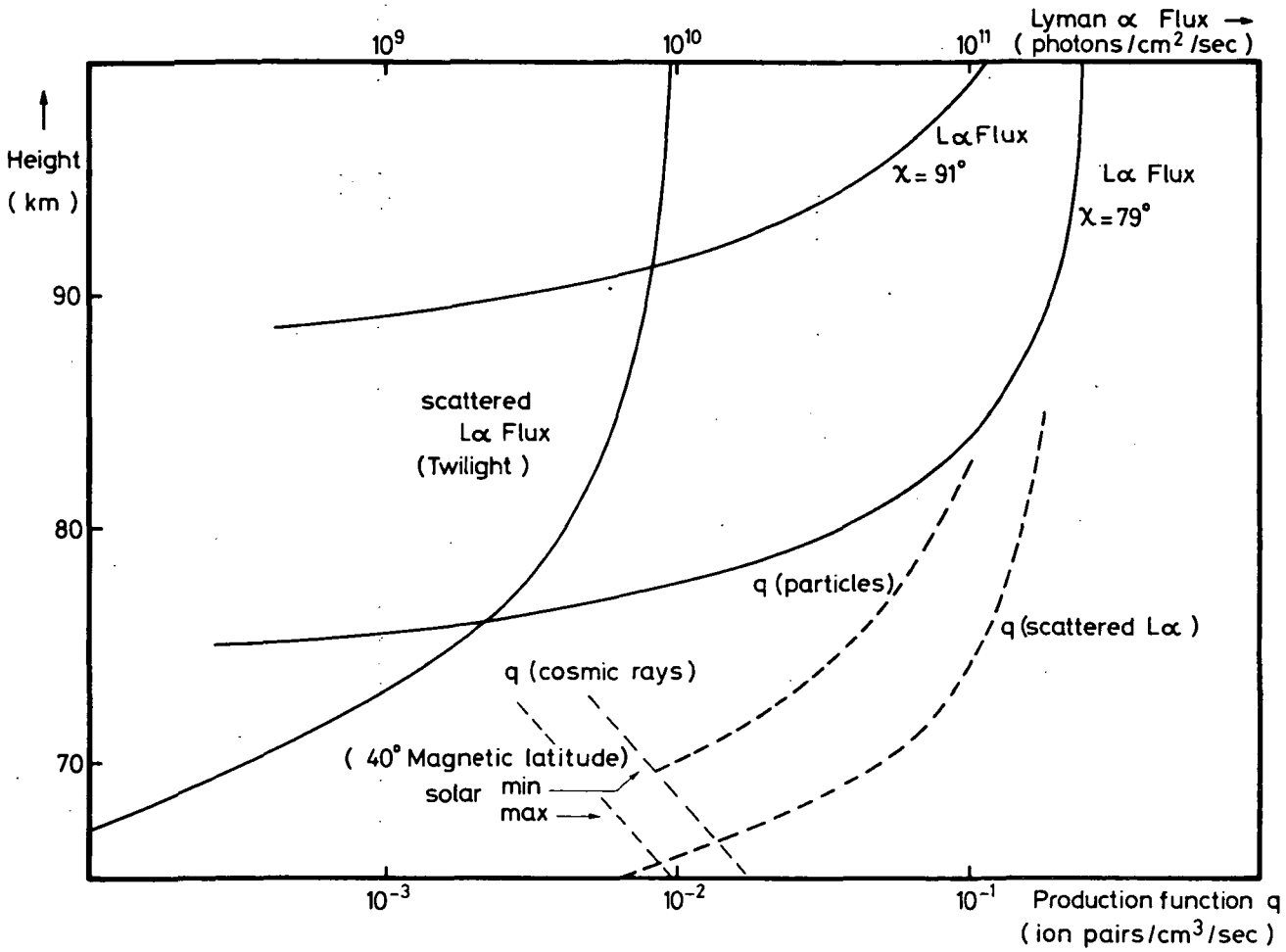

Figure 4. Calculated profiles of direct and scattered Lyman α flux (solid curves). Direct solar Lyman α flux at the top of the atmosphere is taken as 2.7×10^{11} photons cm^{-2} s^{-1}, while the isotropically incident scattered Lyman α flux (at twilight) is taken as 10^{10} photons cm^{-2} s^{-1} (Ref. 15). Ion production (dashed curves) resulting from scattered Lyman α radiation acting on the nitric oxide profile of Meira[14] is compared with ion production by (a) cosmic rays at White Sands (40° magnetic lat., 33° geogr. lat.) and (b) background electron precipitation at similar magnetic latitudes[16] .

4. DISCUSSION

In an attempt to evaluate the positive ion results shown in Figure 2 it is necessary to consider the possible ion production sources operating at our two zenith angles. Aikin[11] has reviewed the present state of knowledge concerning ion production in the lower ionosphere under both day and night conditions. Because of the large nitric oxide concentrations measured in the D-region by Barth[12], Pearce[13] and most recently by Meira[14], it would appear that between 65 and 95 km the Lyman-α/nitric-oxide process is the dominant ion production operating at our two zenith angles. Above 95 km the role of Lyman β and soft X-rays (30-50 Å) cannot be neglected for the $\chi = 79^{\circ}$ case. In figure 4 is shown the altitude dependence of the flux of direct solar Lyman α radiation calculated for the two zenith angles $\chi = 91^{\circ}$ and $\chi = 79^{\circ}$ together with the calculated flux of scattered Lyman α radiation. This latter calculation uses the value of 10^{10} photons cm^{-2} sec^{-1} given by Meier and Mange[15] as the scattered Lyman α flux isotropically incident on the top of the atmosphere at twilight. Also in Figure 4 is shown a comparison of the production functions (q) resulting from (a) cosmic rays, (b) mid-latitude background precipitated electrons (Tulinov[16]) and (c) scattered Lyman α radiation acting on the nitric oxide profile of Meira. In the altitude region below 85 km, the profile of Meira is the most conservative of the three nitric oxide measurements cited above, his values are a factor of 15 below those of Pearce. At 80 km for $\chi = 91^{\circ}$, the combination of $N_+ = 7 \times 10^2$ cm^{-3} and the calculated ion production function (c) yields an upper limit on the ion/ion recombination coefficient from the relation $q/N_+^2 = \alpha_d/\lambda + \alpha_i = 3 \times 10^{-7} \geq \alpha_i$, ($\lambda >> 1$). Laboratory values of small ion/ion recombination coefficients are lower by one to two orders of magnitude[17]. However our upper limit on α_i is not without some meaning, since complex hydrated ions, known to be present in the D-region, would be expected to have higher

combination rates than simple ions. It may also be noted that the effective electron/ion recombination coefficient at 80 km could be as large as 5×10^{-5} (Ref. 18).

The difference between the positive-ion and electron density profiles of Figure 2 we attribute to the presence of negative ions. It is seen that most of the detachments above 75 km take place at zenith angles less than $\chi = 91^{\circ}$. According to the work of Thomas and Bowman[19] the penetration at sunrise of radiation with wavelengths in the band 2100 Å $\leq \lambda \leq$ 3300 Å is controlled by the ozone distribution along the line of sight. The absorption cross section for ozone has a maximum at λ = 2500 Å. Consequently, within this UV band, at a given zenith angle; 2550 Å is the wavelength whose optical depth values occur at the highest altitudes. Figure 5 shows as a function of altitude a plot of the calculated flux of 2550 Å radiation for several zenith angles. These calculations are affected by the ozone distribution above 70 km, which at sunrise is itself a rapidly changing function of zenith angle. The ozone distributions used for the different zenith angles of Figure 5 were taken from calculations by A.C. Aikin[20]. Also shown in Figure 5 is a re-plot of

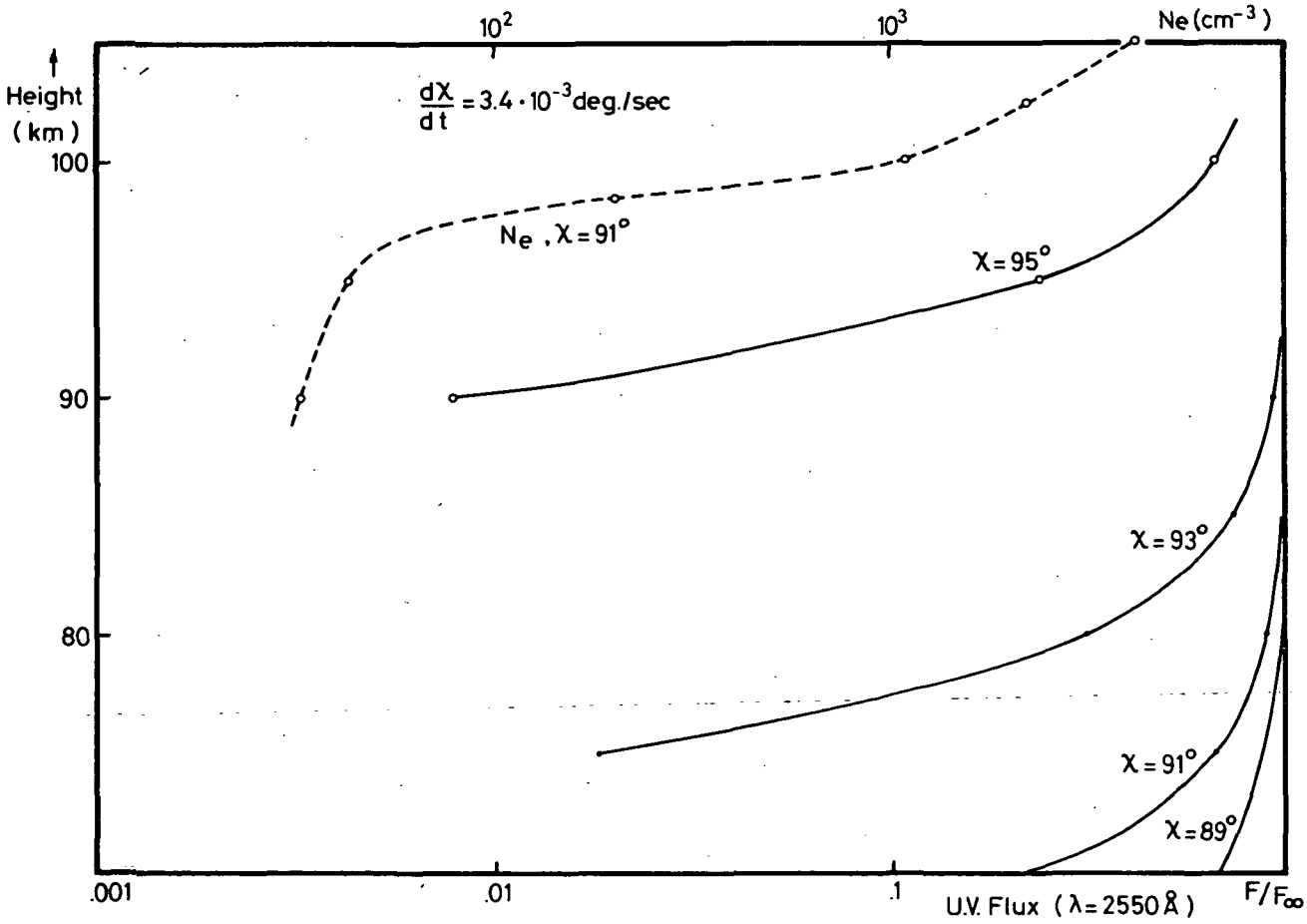

Figure 5. Calculated profiles of 2550 Å flux (solid curves) for several solar zenith angles. Dashed curve shows electron density profile measurement at $\chi = 91^{\circ}$.

the electron density measured on our rocket shot at $\chi = 91^{\circ}$. At the time of the rocket shot the zenith angle was changing at the rate $d\chi/dt = 3.4 \times 10^{-3}$ degrees s^{-1}. We can then see by inspection of Figure 5 that the profile of the UV flux and the electron density profile are similar in shape but separated by more than 4 degrees of zenith angle (i.e. by more than 20 minutes in time). Other wavelengths in the UV band will yield curves similar to those of Figure 5 but having even greater time separation with the electron-density profile.

Figure 6 shows as a function of altitude a plot of the calculated flux of Lyman α radiation for several zenith angles together with the electron density measured at $\chi = 91^{\circ}$. Here we can see that the Lyman α and electron-density profiles are also similar in shape, but in this case separated by about one degree of zenith angle (i.e. a delay of about 5 minutes). Unfortunately, until both the negative ion's identity and photodetachment cross section *versus* wavelength are known, there is no reason to prefer one value of the time delay. Hence it is clear that the question of which wavelength is responsible for the observed detachment cannot be decided at this time.

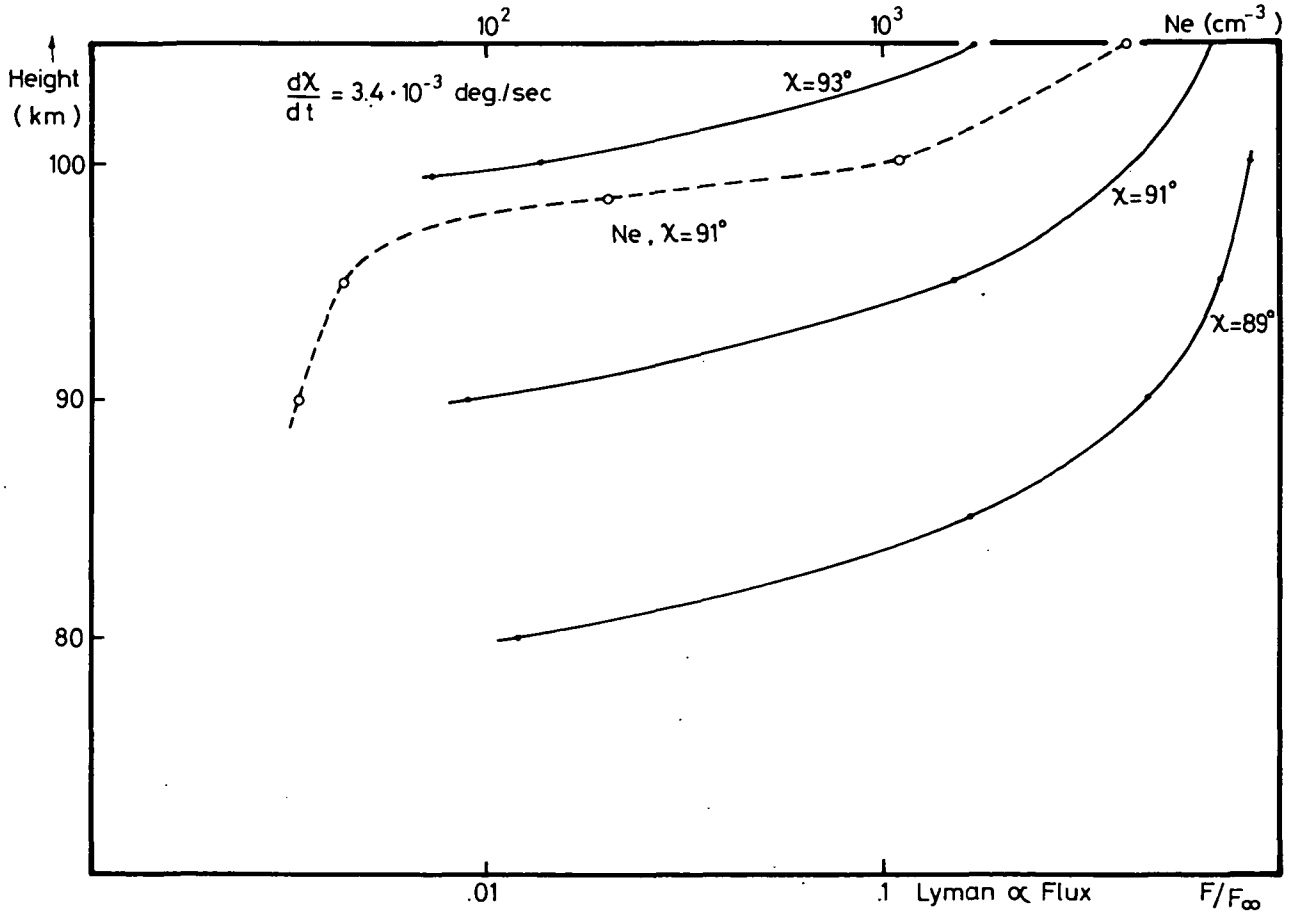

Figure 6. Calculated profiles of Lyman α flux (solid curves) for several solar zenith angles. Dashed curve shows electron-density profiles measured at $\chi = 91^{\circ}$. In Figures 5 and 6, solar zenith angle changes at a rate $d\chi/dt = 3.4 \times 10^{-3}$ degrees s^{-1}.

5. CONCLUSIONS

In this report we have tried to bring out the following three points:

1) Negative ions at sunrise are important at least as high as 95 km.

2) Scattered Lyman α radiation is probably the dominant source of a significant positive-ion density (i.e. $\gtrsim 10^2$ cm^{-3}) in the pre-sunrise D-region at White Sands.

3) It is not possible to associate the detachment of negative ions at sunrise with any particular wavelength of radiation until both the negative ion's identity and photodetachment cross section versus wavelength are known.

ACKNOWLEDGEMENTS

We are especially grateful to J.E. Jackson (GSFC) for his ionogram analyses, upon which our rocket trajectories are based.

The very helpful ozone calculations of A.C. Aikin (GSFC) are also gratefully acknowledged.

REFERENCES

1) Smith, R.A., Proceedings of conference on ground-based radio wave propagation studies of lower ionosphere.
DRTE Ottawa, April 1966.

2) Thomas, L. & Harrison, M.D., The electron density distributions in the D-region during the night and pre-sunrise period.
J. Atmos. Terr. Phys. 32, 1, 1970.

3) Bowhill, S.A. & Smith, L.G., Rocket measurements of the lowest ionosphere at sunrise and sunset.
Space Research VI, 511, 1966, MacMillan & Co. Ltd. London.

4) Sechrist, C.F., Interpretation of pre-sunrise electron densities and negative ions in the D-region.
J. Atmos. Terr. Phys. 30, 371, 1968.

5) Fehsenfeld, F.C., Schmeltekopf, A.C., Schiff, H.I. & Ferguson, E.E., Laboratory measurements of negative ion reactions of atmospheric interest.
Planet. Space Sci. 15, 373, 1967.

6) Sonin, A.A., Theory of ion collection by a supersonic atmospheric sounding rocket.
J. Geophys. Res. 72, 4547, 1967.

7) Kane, J.A. & Troim, J., Rocket measurements of D-region electron number densities at sunrise.
J. Geophys. Res. 72, 1118, 1967.

8) Hale, L.C., Hoult, D.P. & Baker, D.C., A summary of blunt probe theory and experimental results.
Space Research VIII, 320, 1968. North Holland Publishing Co.

9) Folkestad, K., Landmark, B., Skovli, G. & Kane, J.A., Results of rocket measurements in the lower auroral ionosphers.
J. Atmos. Terr. Phys. 32, 835, 1969.

10) Jespersen, M., Kane, J.A. & Landmark B., Electron and positive ion density measurements during conditions of auroral absorption.
J. Atmos. Terr. Phys. 30, 1955, 1968.

11) Aikin, A.C., The ion pair production function of the lower ionosphere.
NASA X-615-69-490, 1969.

12) Barth, C.A., Nitric oxide in the upper atmosphere.
Annls. Géophys. 22, 198, 1966.

13) Pearce, J.B., Rocket measurement of nitric oxide between 60 and 96 km.
J. Geophys. Res. 74, 853, 1969.

14) Meira, L.G., Rocket measurements of upper atmospheric nitric oxide and their consequences to the lower ionosphere.
Ph.D. Thesis Univ. of Colorado, 1970.

15) Meier, R.R. & Mange, P., Geocoronal hydrogen: an analysis of the Lyman-alpha airglow observed from OGO 4.
Planet. Space Sci. 18, 803, 1970.

16) Tulinov, V.F., On the role of corpuscular radiation in the formation of the lower ionosphere.
Space Research VII, North Holland Publ. Co., 386, 1967.

17) Loeb, L., Basic processes of gaseous electronics.
Univ. of California Press, Berkeley, 1960.

18) Reid, G.C., Production and loss of electrons in the quiet daytime D-region of the ionosphere.
J. Geophys. Res. 75, 2551, 1970.

19) Thomas, L. & Bowman M.R., Atmospheric penetration of ultraviolet and visible solar radiations during twilight periods.
J. Atmos. Terr. Phys. 31, 1311, 1969.

20) Aikin, A.C., Private communication.

APPENDIX

Rocket trajectory

Owing to a radar failure it was necessary to determine the rocket trajectory by the following indirect method. Peak time is accurately determined as the time at which maximum Faraday rotation is observed and from symmetry in ion current versus time. With the aid of predicted rocket-performance data a reasonable peak altitude is then assigned to the observed peak time. On the basis of the resulting trajectory, an electron-density profile is deduced from the Faraday rotation experiment. From this electron-density profile, a unique virtual height ionogram can be computed. This computed ionogram is then compared with the real White Sands ionogram taken close to the time of rocket launch. The rocket peak altitude is then adjusted until the best agreement is obtained between computed virtual heights and altitudes at which ionogram echoes are observed.

It is estimated that with the high-quality ionograms available in our present case, our final trajectories are accurate to within $\pm$ 3 km.